ORIGINAL ARTICLE

Highly Dispersed Pt Nanoparticles Root in Single-Atom Fe Sites in LDHs toward Efficient Methanol Oxidation

Qing-Cheng Meng [a,#], Lin-Bo Jin [a,#], Meng-Ze Ma [a], Xue-Qing Gao [b], Ai-Bing Chen [b,*], Dao-Jin Zhou [a,*], Xiao-Ming Sun [a,*]

[a] State Key Laboratory of Chemical Resource Engineering, Beijing Advanced Innovation Center for Soft Matter Science and Engineering, Beijing University of Chemical Technology, Beijing, 100029, China
[b] College of Chemical and Pharmaceutical Engineering, Hebei University of Science and Technology, Shijiazhuang, 050018, China

Abstract

Active and durable electrocatalysts for methanol oxidation reaction are of critical importance to the commercial viability of direct methanol fuel cell, which has already attracted growing popularities. However, current methanol oxidation electrocatalysts fall far short of expectations and suffer from excessive use of noble metal, mediocre activity, and rapid decay. Here we report the Pt anchored on NiFe-LDHs surface hybrid for stable methanol oxidation in alkaline media. Based on the high intrinsic methanol oxidation activity of Pt nanoparticles, the substrates NiFe-LDHs further enhanced anti-poisoning ability and maintained unaffected stability after 200,000 s cycle test compared to commercial Pt/C catalyst. The use of NiFe-LDHs is believed to play the decisive role to evenly disperse Pt nanoparticles on their surface using single atomic dispersed Fe as anchoring sites, making full use of abundant OH groups and subsequent facilitating the oxidative removal of carbonaceous poison on neighboring Pt sites. This work highlights the specialty of NiFe-LDHs in improving the overall efficiency of methanol oxidation reaction.

Keywords: Layered double hydroxides; Methanol oxidation; Single-atom; Pt electrocatalysts

1. Introduction

Growing concerns regarding the climate change and regional energy disputes have arouse attention worldwide in finding renewable and clean energy to ensure the sustainable development of society [1,2]. Direct methanol fuel cells (DMFCs) have long been considered as a promising power conversion tool by virtue of their higher energy-conversion rate, wide working temperature range, no pollution emissions, portability and safety of raw materials [3—6]. However, it is still challenging to realize the mass commercialization, mainly originating from high overpotential at an anode (where methanol is oxidized, requiring hundreds of mV as overpotential [7—9]), unaffordable cost associated with precious metal electrocatalysts (for example, Pt) and low operation durability of the anode operation [10—12] (carbonaceous species poisoning). In consideration of high cost and scarcity, exposing more accessible surface area by reducing size of Pt is an essential and a direct approach for achieving the commercialization of DMFCs, however, the limited durability is always observed due to the aggregation of nanoparticles (NPs) or the poisoning of noble metals [13—16]. Hence, desirable supporting materials with large surface area that can anchor and disperse the Pt NPs are necessary to be developed and optimized. In recent years, many materials have been utilized

Received 28 June 2022; Received in revised form 19 July 2022; Accepted 20 September 2022
Available online 26 September 2022

* Corresponding author, Ai-Bing Chen, Tel: (86-311)88668375, E-mail address: chen_ab@163.com.
* Corresponding author, Dao-Jin Zhou, Tel: (86-10)64448751, E-mail address: zhoudj@mail.buct.edu.cn.
* Corresponding author, Xiao-Ming Sun, Tel: (86-10)64448751, E-mail address: sunxm@mail.buct.edu.cn.
[#]These authors contribute equally to this work.

https://doi.org/10.13208/j.electrochem.2215007

as supporting materials for loading of Pt-based nanocatalysts, including metal oxides and nanocarbon materials [11,17−19], while only limited improvements in durability have been achieved so far, presumably due to the limited capability of the supports to assist in the oxidative removal of CO on adjacent Pt sites, and the weak interaction between Pt and supports fails preventing the aggregation of Pt during methanol oxidation [20−22].

In seeking optimal supports, which can anchor and stabilize the noble metal NPs, and facilitate the removal of CO during methanol oxidation on noble metal NPs, two-dimensional metal hydroxides have been intensively investigated. On the one hand, the metal hydroxides possess high specific surface area and rich sites for noble metal anchoring, on the other hand, the metal hydroxides shall supply abundant OH during methanol oxidation to benefit the oxidation of CO [23−25]. For example, Li and Cai et al. successively reported the use of $Ni(OH)_2$ to disperse Pt and Pd NPs for methanol oxidation, showing enlarged electrochemical surface area and excellent working stability, which have proven to improve the overall methanol oxidation efficiency [11]. While the combination of noble metal with metal hydroxides is attracting and proving effective in methanol oxidation, further advancements such as facilitating the generation of OH_{ads} to improve the intrinsic activity and selectivity, achieving high dispersion of noble metals via strong support-metal interaction, are still vacant based on unitary metal hydroxides. Layered double hydroxides (LDHs), in which partial M^{2+} ions in laminates are replaced by M^{3+} ions via isomorphous substitution, while all the M^{3+} will be isolated from each other by electrostatic repulsion force, have shown potential in addressing above problems [26,27]. Firstly, fast generation of OH_{ads}, which can be used to oxidize adsorbed intermediates of methanol oxidation, on LDHs can be facilitated via compositional modulation, this process has already shown in oxygen evolution reaction [28−31]. Secondly, the partial substitution of M^{2+} by M^{3+} results in unbalanced charge configuration, which will directionally adsorb noble metal precursors to specific sites and form strong electrostatic attraction interaction between M^{3+}−O(H)−Pt [32], resulting in the uniformly dispersed and stable decoration of anchored noble metal. Thirdly, OH^- transfer is favorable on LDHs with large surface area (generally over 120 $m^2 \cdot g^{-1}$), which can relive the local pH evolution around the surface of electrode and protect the electrode from reconstruction, especially at high current density [32,33].

In this work, Pt NPs with acknowledged methanol oxidation activity and NiFe-LDHs with excellent OH_{ads} generation capability are combined together by a two-step synthetic process, in which the single-atomic dispersed Fe^{3+} ions in LDHs laminates serve as anchoring sites for Pt precursors, ensuring the highly dispersion of Pt. Electrochemical characterizations for activity, selectivity and stability jointly confirm the positive effect from NiFe-LDHs in facilitating methanol oxidation, avoiding CO poison or Pt aggregation by showing the onset potential at −0.64 V vs. SCE and no obvious decay after the cycle test for 200,000 s. This work shall inspire the deep understanding in characteristic of LDHs, and optimization of LDHs with noble metal NPs toward efficient methanol oxidation.

2. Results and discussion

The Pt/NiFe-LDHs electrocatalysts were synthesized by an electrostatic interaction-based self-assembly strategy, which is illustrated in Fig. 1. Firstly, the NiFe-LDHs nanosheets were synthesized by co-precipitation method. After adding H_2PtCl_6 into LDHs suspensions (LDHs nanosheets were dispersed and stirred for over 72 h), $PtCl_6^{2-}$/LDHs composite was formed as a result of the electrostatic attraction between $PtCl_6^{2-}$ and LDHs nanosheets, as shown in Fig. 1. Finally, the addition of sodium borohydride reduced the $PtCl_6^{2-}$/NiFe-LDHs hybrids to Pt/NiFe-LDHs hybrids [34]. A low concentration of H^+ plays two roles: firstly, H^+ can react with surface OH groups to open unsaturated coordinated Fe sites for $PtCl_6^{2-}$ adsorption; secondly, H^+ would controllably etch (by the modulation of H_2PtCl_6 addition) LDHs nanosheets to induce defective metal hydroxides nanostructure in the Pt/NiFe-LDHs hybrids. These defects are also believed to play a decisive role in promoting the transformation from adsorbed OH^- species to OH_{ads} at applied potentials and subsequent oxidative removal of carbonaceous poison on neighboring Pt sites [35,36].

The morphology and nanostructure of NiFe-LDHs were characterized by scanning electron microscopy (SEM, Figure S1) and transmission electron microscopy (TEM, Figure S2). It can be observed that the NiFe-LDHs have a flake-like morphology with lateral sizes in a range of 50−100 nm. XRD patterns of NiFe-LDHs are shown in Figure S3. The diffraction peaks at 2θ = 11.4°, 23.0°, 34.4°, 39.0°, 46.0°, 59.9°and 61.3° are attributed to the (003), (006), (012), (015), (018), (110) and (113) planes, which are in accordance with that reported in the earlier literatures [37].

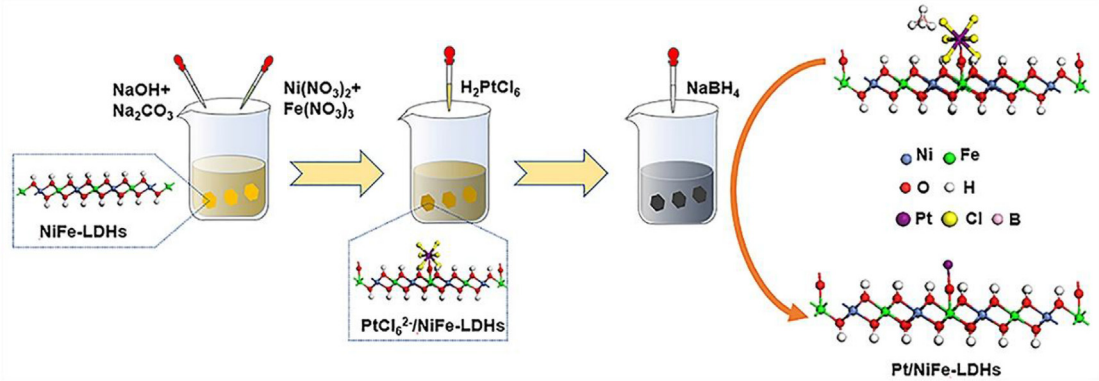

Fig. 1. Schematic illustration showing the preparation process of the Pt/NiFe-LDHs.

Fig. 2a and b shows the TEM images of Pt/NiFe-LDHs and commercial Pt/C, respectively. Notably, the Pt NPs loaded on NiFe-LDHs nanosheets show high uniformity and smaller particle size compared with the Pt on carbon support, highlighting that the electrostatic interaction between Pt NPs and single-atomic dispersed Fe^{3+} in LDHs laminates makes a real difference in dispersing the Pt NPs, and by the first-principles calculations (Figure S4) we confirm that the adsorption energy of Pt on Fe^{3+} sites (Pt−O−Fe^{3+}) is lowered than that on Ni^{2+} sites (Pt−O−Ni^{2+}). The high-resolution TEM (HR-TEM) images exhibit an interplanar spacing of 0.22 nm and 0.25 nm for the (111) plane of the Pt NPs and (012) plane of the LDHs, respectively (Fig. 2c). The XRD patterns of Pt/NiFe-LDHs electrocatalyst are presented in Fig. 2d and S5, and the diffraction peaks locate at 2θ values of 39.8°, 46.2° and 67.5°, corresponding to (111), (200) and (220) planes, respectively, of a pure face-centered cubic structure of Pt [38]. Similar LDHs diffraction peaks prove that the crystalline structure of NiFe-LDHs has not been altered upon Ni: Fe ratios or the deposition of Pt NPs, which can also be observed from the SEM images in Figure S6, confirming the successful synthesis of the Pt/NiFe-LDHs electrocatalysts.

Cyclic voltammetry (CV) was used to study the electrochemical performance of the electrocatalysts in MOR. Data in Fig. 3a display an intense anodic

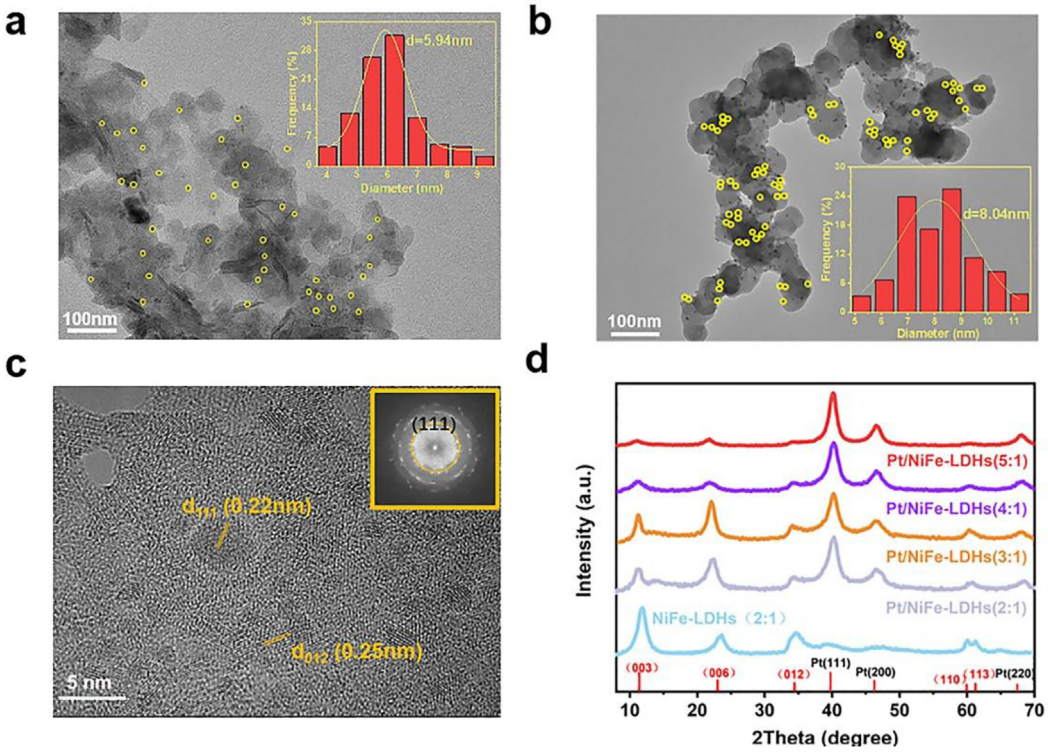

Fig. 2. TEM images of (a) the Pt/NiFe-LDHs and (b) the commercial Pt/C, (c) HRTEM image and (d) XRD patterns of the Pt/NiFe-LDHs.

peak in the forward scan and a minor anodic peak in the reverse scan. The anodic peak in the forward scan is ascribed to the oxidation of methanol to CO_2, while another one in the reverse scan is ascribed to the oxidized removal of the CO and other carbonaceous species generated on Pt in the forward scan [39]. In addition, the ratio of forward-to-backward oxidation current, I_f/I_b, is an important parameter evaluating the electrocatalyst tolerance to CO and other poisoning carbonaceous species. A higher value demonstrates that the oxidative removal of the poisoning carbonaceous species on the electrocatalyst surface is more favorable. Fig. 3a and b study and compare the methanol oxidation reaction (MOR) activity and selectivity of Pt/NiFe-LDHs with different Ni:Fe ratios, from which a conclusion can be brought that the Pt/Ni_3Fe_1-LDHs have the best electrocatalytic ability on MOR according to the exceptional current (3.41 mA), high I_f/I_b (2.84) and low onset potential (−0.64 V vs. SCE). Since OH_{ads} species are both actively involved in MOR and oxygen evolution, the results in this work agree with previous research that Ni_3Fe_1-LDHs have advantages in generating OH_{ads} [26], which are helpful in facilitating the oxidative removal of the poisoning carbonaceous species. The proposed MOR mechanism on Pt/NiFe-LDHs is shown in Figure S7. Firstly, atomic-dispersed Fe sites in LDHs help to disperse anchored Pt nanoparticles, resulting in the more exposed electrochemical surface area of Pt. Secondly, the oxidation of methanol can always lead to the tight adsorption of CO on the surface of Pt, while the OH_{ads} as generated on the surface of LDHs would facilitate the fast removal of CO species, resulting in long-term durability. CO stripping experiments were also used to probe the strong resistance of Pt/NiFe-LDHs to CO poisoning. As shown in Figure S8, the CO oxidation peak of Pt/NiFe-LDHs has a negative shift compared to that of Pt/C, and the integrated area for CO oxidation is also smaller on Pt/NiFe-LDHs than on Pt/C, indicating that the adsorption of CO on Pt/NiFe-LDHs is weaker than that on Pt/C.

Fig. 3c and d further study the influence of loading Pt contents on the MOR performance of the hybrid electrocatalysts. Obviously, Pt(16%)/Ni_3Fe_1-LDHs exhibited an optimal performance with the highest current of about 15 mA, locating at the apex of Pt content-MOR activity volcano plot. At the beginning of the MOR, the methanol will be adsorbed on Pt as the active site, so the increased

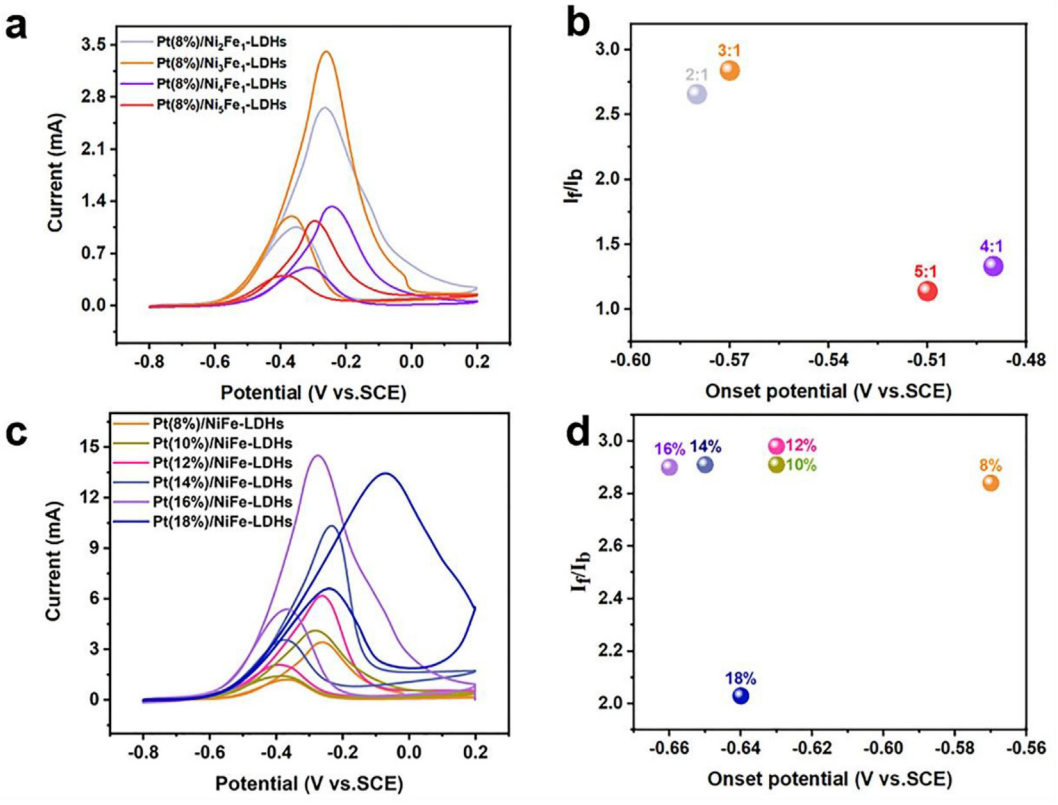

Fig. 3. (a) CV curves, (b) I_f/I_b and onset potential of Pt(8%)/NiFe-LDHs at different Ni:Fe ratios measured in N_2-saturated 1 mol·L^{-1} CH_3OH solution containing 1 mol·L^{-1} KOH at a scan rate of 50 mV·s^{-1}, (c) CV curves, (d) I_f/I_b and onset potential of Pt/Ni_3Fe_1-LDHs loaded by different amounts of H_2PtCl_6 measured in N_2-saturated 1 mol·L^{-1} CH_3OH solution containing 1 mol·L^{-1} KOH at a scan rate of 50 mV·s^{-1}.

content of Pt will be favor for the adsorption of methanol, resulting the growing MOR current, however when the content of Pt is too high, the aggregation of Pt NPs is inevitable, thereby reducing its active specific surface area and leading to excessive adsorption of carbonaceous by-products during MOR, finally causing the declines of MOR activity and selectivity. Therefore, the MOR activity of the Pt(16%)/Ni_3Fe_1-LDHs stands out among all composites.

Lately, the Pt valence state, which is tightly related to the adsorption energies of methanol and CO intermediates on Pt during MOR, was studied by X-ray photoelectron spectroscopy (XPS) in Figure S9. Firstly, the Pt $4f_{7/2}$ binding energies of the Pt/NiFe-LDHs are down-shifted compared to that of commercial Pt/C, which indicates the change in the electron density of Pt due to electrostatic interaction in Pt—O—Fe^{3+}. Furthermore, the ratio between Pt^{2+}/Pt^0 decreases in Pt/NiFe-LDHs compared with that in Pt/C, verifying the drop of Pt valence state in Pt/NiFe-LDHs. The increase of electro density of Pt can possibly weaken the adsorption of reaction intermediates, here is CO, on the electrocatalyst surface, and in turn enhance the selectivity of MOR [40—43]. The high-resolution Ni 2p spectrum (Figure S10a) shows two peaks with binding energies at 856.4 and 874.1 eV correspond to the Ni^{2+} $2p_{3/2}$ and Ni^{2+} $2p_{1/2}$, respectively, which is in good agreement with a previous report [44]. The Fe 2p signal is composed of two peaks (Figure S10b), belonging to Fe $2p_{1/2}$ and Fe $2p_{3/2}$ binding energies of the Fe oxidation state (Fe^{3+}) [45]. Compared the valence states of Ni and Fe between the NiFe-LDHs and Pt/NiFe-LDHs, we could find that there is no difference between the nickel element, while the binding energy of iron decreases slightly from 712.95 eV to 712.6 eV after Pt anchoring. This result can be understood as since Pt^{4+} is preferentially reduced by the sodium borohydride [46], the adjacent Fe^{3+} is also partially reduced, further confirming the strong interaction between Pt and Fe by establishing Pt—O—Fe^{3+} bond on NiFe-LDHs surface.

The mass activity of Pt-based catalysts is usually used for evaluating the MOR catalytic properties, which is calculated by the peak current per milligram Pt. According to Fig. 4a, the mass activity of the Pt(16%)/Ni_3Fe_1-LDHs toward MOR is as high as 999 $mA \cdot mg_{Pt}^{-1}$, which is 1.23 times higher than that of commercial Pt/C (781 $mA \cdot mg_{Pt}^{-1}$) and 1.22 times higher than that of benchmark Pt/$Ni(OH)_2$ (820 $mA \cdot mg_{Pt}^{-1}$). Then, we performed 1200 cycles CVs to investigate the frequent switch on/off durability of the electrocatalyst during MOR. Also exhibited in Fig. 4a, the peak current density degenerates with prolonged cycling time. This phenomenon could be ascribed to the continuous generation of intermediates and their poisoning impacts on electrocatalyst during MOR, also including the detachment of Pt NPs from the substrate or the aggregation of Pt NPs. The peak current densities for commercial Pt/C, Pt/$Ni(OH)_2$ and Pt(16%)/Ni_3Fe_1-LDHs after the 1200^{th} cycle were about 48.78 $mA \cdot mg_{Pt}^{-1}$, 350.25 $mA \cdot mg_{Pt}^{-1}$, 608 $mA \cdot mg_{Pt}^{-1}$, respectively, which is 6.2%, 42.7% and 60% of the first cycle, respectively, highlighting the positive effect of NiFe-LDHs in facilitating the oxidation of methanol, accelerating the removal of carbonaceous by-products, and anchoring the Pt NPs against aggregation.

The continuous working stability is also an important index to evaluate the catalytic performance of MOR electrocatalysts. By using amperometric *i-t* method, we firstly characterized the short-term stability of electrocatalyst. As shown in Fig. 4b, three electrocatalysts display a current density decline in the initial period, perhaps resulting from electrocatalyst poisoning by chemisorbed carbonaceous species formed during the methanol oxidation. At the end of stability test, the current density of Pt(16%)/Ni_3Fe_1-LDHs electrocatalyst was higher than those of commercial Pt/C and Pt/$Ni(OH)_2$, further confirming the excellent working stability of Pt(16%)/Ni_3Fe_1-LDHs.

Then the long-term operation durability of these two electrocatalysts were characterized and are compared. At the end of continuous operation for 50,000 s, negligible activities (almost no MOR working current densities) maintained for commercial Pt/C (Figure S11). In stark contrast, Pt(16%)/Ni_3Fe_1-LDHs still delivered a current density of 145 $mA \cdot mg_{Pt}^{-1}$, accounting for 33% of initial working current density. To our surprise, we found that Pt(16%)/Ni_3Fe_1-LDHs could still exhibit the initial MOR activity in a fresh electrolyte after working for 50,000 s, while Pt/C could not recover to the initial activity (merely recovered to around 30% as shown in Figure S11). We repeated the cycling up to four times for a total of 200,000 s, and the full activity was recovered every time (Figure S11). So, the drop of the MOR working current density of Pt(16%)/Ni_3Fe_1-LDHs may be mainly induced by the changes of pH and composition of electrolyte (generated CO_2 being dissolved in KOH, resulting in the formation of K_2CO_3 and drop of electrolyte pH), rather than the severe reconstruction or the aggregation of Pt NPs in Pt(16%)/Ni_3Fe_1-LDHs.

To supply experimental evidence for the greatly enhanced durability of the Pt(16%)/Ni_3Fe_1-LDHs as compared to that of the commercial Pt/C in MOR, we further monitored their morphological

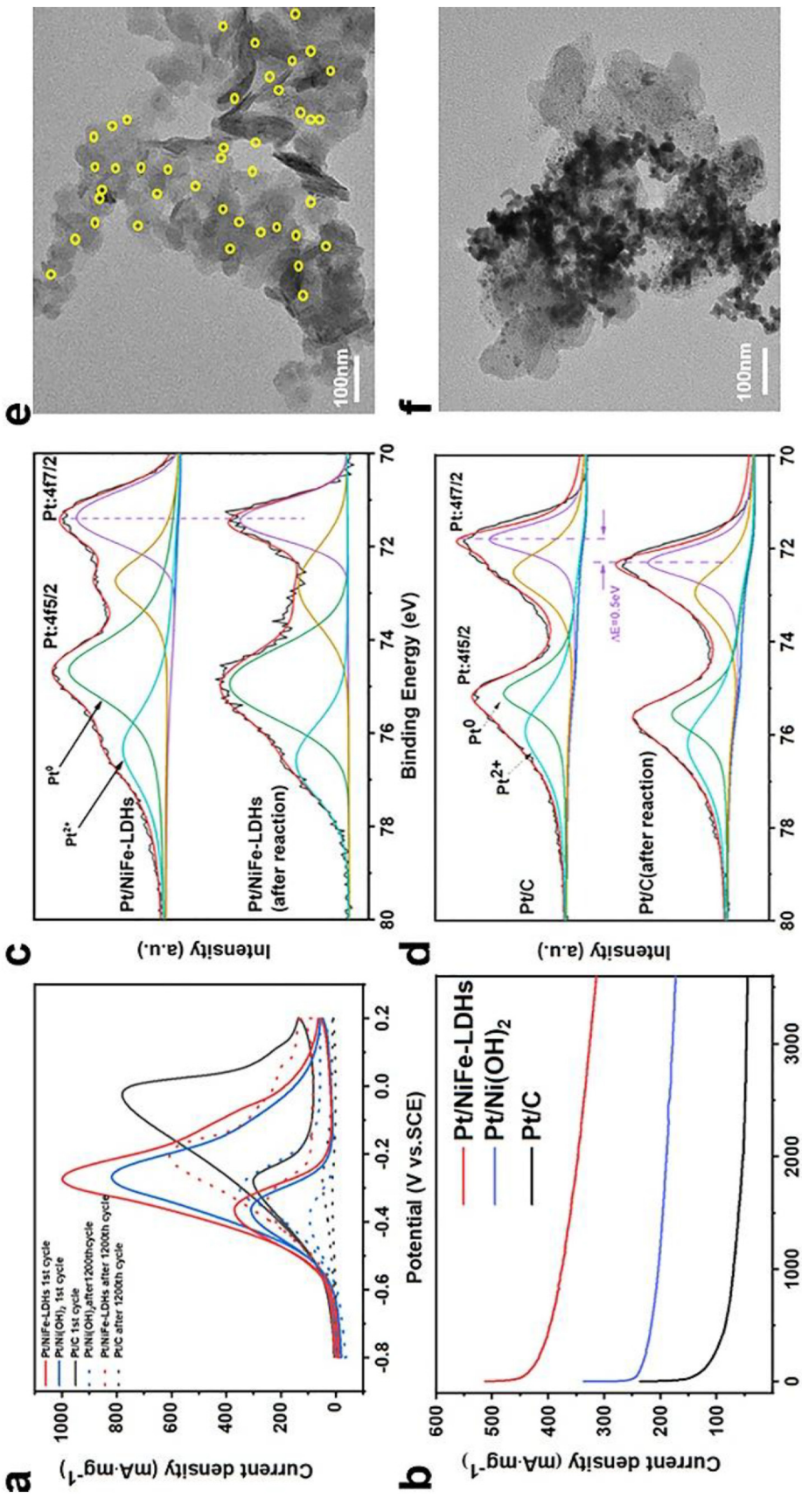

Fig. 4. (a) CV and (b) chronoamperometric (CA) curves of Pt/NiFe-LDHs, Pt/C and Pt/Ni(OH)$_2$ at different cycle numbers measured in N_2-saturated 1 mol·L^{-1} CH_3OH solution containing 1 mol·L^{-1} KOH at a scan rate of 50 mV·s^{-1}; Pt 4f XPS spectra of Pt/NiFe-LDHs, (c) and Pt/C, (d) after MOR reaction; TEM images of Pt/NiFe-LDHs (e) and Pt/C (f) after MOR reaction.

and compositional changes after the durability test. XPS spectra were used to monitor the evolution of the element composition and electronic states of Pt(16%)/Ni_3Fe_1-LDHs and Pt/C during the long-term stability test. The results indicate that the electronic states of Ni and Fe in Pt(16%)/Ni_3Fe_1-LDHs were well maintained (Figure S12), also negligible shifts of Pt binding energy can be observed in Fig. 4c. In contrast, the Pt binding energies of the commercial Pt/C were up-shifted 0.5 eV after reaction (Fig. 4d). The Pt^{2+}/Pt^0 ratio as compared in Fig. 4c exhibits that no obvious Pt oxidation could be observed in Pt(16%)/Ni_3Fe_1-LDHs, while a growing value of Pt^{2+}/Pt^0 ratio could be detected in Pt/C, indicating the transformation from Pt^0 to Pt^{2+} during MOR, so it is reasonable that the activity of Pt/C decayed after prolonged working hours. Moreover, it is found that the Pt NPs in Pt(16%)/Ni_3Fe_1-LDHs maintained their morphology and dispersion well during the 200,000 s stability test (Fig. 4e). In the case of the commercial Pt/C, an obvious aggregation and ripening of Pt NPs can be observed (Fig. 4f).

The interactions between Pt NPs and NiFe-LDHs have merits in providing sufficient OH_{ads} for the oxidation of methanol and carbonaceous by-products, requiring low Pt loading by maximizing the available surface area of Pt NPs, anchoring Pt NPs via Fe^{3+}—O—Pt bond against Pt aggregation during MOR procedure. In real DMFC devices, it would be highly desirable for MOR electrocatalysts with low Pt loading, high activity, and reactivated during operation breaks by simply replacing the electrolyte by fresh ones, the electrocatalyst reported in this work suits well to the requirements.

3. Conclusions

In summary, uniform and small Pt nanoparticles were loaded on the NiFe-LDHs nanosheets and used as a high-efficient MOR electrocatalyst. The presence of NiFe-LDHs dramatically promoted the electrocatalytic performance of Pt for the MOR in an alkaline solution by evenly dispersing Pt nanoparticles on their surface via Fe—O(H)—Pt bonding, promoting the generation of OH_{ads} and subsequent oxidative removal of carbonaceous poison on neighboring Pt sites. Through the synergistic effect between Pt and NiFe-LDHs, our electrocatalyst retained an exceptional mass activity of 145 $mA \cdot mg^{-1}$ even after 50,000 s chronoamperometric measurement, and it could rework functionally in replaced fresh electrolytes. Finally, the resulting Pt/NiFe-LDHs electrocatalyst exhibited higher electrocatalytic activity (onset potential at −0.64 V vs. SCE) and better anti-poisoning ability comparing to commercial Pt/C catalyst. This study implies that the Pt/NiFe-LDHs electrocatalyst has great potential applications in methanol fuel cell, which are essential for the clean development of society.

Acknowledgements

This work was financially supported by the National Natural Science Foundation of China (21935001, 22175012, 22005022), the S&T Program of Hebei (21344601D), the Beijing Natural Science Foundation (2214062), the Program for Changjiang Scholars and Innovation Research Team in the University (No. IRT1205), the Fundamental Research Funds for the Central Universities, and Beijing Advanced Innovation Center for Soft Matter Science and Engineering is acknowledged as well.

References

[1] Shao M F, Ning F Y, Zhao J W, Wei M, Evans D G, Duan X. Hierarchical layered double hydroxide microspheres with largely enhanced performance for ethanol electrooxidation [J]. Adv. Funct. Mater., 2013, 23(28): 3513−3518.
[2] Xu C W, Wang H, Shen P K, Jiang S P. Highly ordered Pd nanowire arrays as effective electrocatalysts for ethanol oxidation in direct alcohol fuel cells[J]. Adv. Mater., 2007, 19(23): 4256−4259.
[3] Arico A S, Srinivasan S, Antonucci V. DMFCs: from fundamental aspects to technology development[J]. Fuel Cell, 2001, 1(2): 133−161.
[4] Zhao X, Yin M, Ma L, Liang L, Liu C P, Liao J H, Lu T H, Xing W. Recent advances in catalysts for direct methanol fuel cells[J]. Energy Environ. Sci., 2011, 4(8): 2736−2753.
[5] Wasmus S, Küver A. Methanol oxidation and direct methanol fuel cells: a selective review[J]. J. Electroanal. Chem., 1999, 461(1−2): 14−31.
[6] Yang C C, Chiu S J, Chien W C. Development of alkaline direct methanol fuel cells based on crosslinked PVA polymer membranes[J]. J. Power Sources., 2006, 162(1): 21−29.
[7] Li Z H, Shao M F, An H L, Wang Z X, Xu S M, Wei M, Evans D G, Duan X. Fast electrosynthesis of Fe-containing layered double hydroxide arrays toward highly efficient electrocatalytic oxidation reactions[J]. Chem. Sci., 2015, 6(11): 6624−6631.
[8] Yu E H, Scott K, Reeve R W. A study of the anodic oxidation of methanol on Pt in alkaline solutions[J]. J. Electroanal. Chem., 2003, 547(1): 17−24.
[9] Qi L, Yin Y, Shi W Y, Liu J G, Xing D M, Liu F Q, Hou Z J, Gu J, Ming P W, Zou Z G. Intermittent microwave synthesis of nanostructured Pt/TiN-graphene with high catalytic activity for methanol oxidation[J]. Int. J. Hydrog. Energy., 2014, 39(28): 16036−16042.
[10] Yang J, Hübner R, Zhang J W, Wan H, Zheng Y Y, Wang H L, Qi H Y, He L Q, Li Y, Dubale A A, Sun Y J, Liu Y T, Peng D L, Meng Y Z, Zheng Z K, Rossmeisl J, Liu W. A robust PtNi nano frame/N-doped graphene aerogel electrocatalyst with both high activity and stability[J]. Angew. Chem., Int. Ed., 2021, 60(17): 9590−9597.
[11] Huang W J, Wang H T, Zhou J G, Wang J, Duchesne P N, Muir D, Zhang P, Han N, Zhao F P, Zeng M, Zhong J, Jin C H, Li Y G, Lee S T, Dai H J. Highly active and durable methanol oxidation electrocatalyst based on the synergy of

platinum-nickel hydroxide-graphene[J]. Nat. Commun., 2015, 6: 10035.

[12] Reddington E, Sapienza A, Gurau B, Viswanathan R, Sarangapani S, Smotkin E S, Mallouk T E. Combinatorial electrochemistry: a highly parallel, optical screening method for discovery of better electrocatalysts[J]. Science, 1998, 280(5370): 1735−1737.

[13] Tso C P, Zhung C M, Shih Y H, Tseng Y M, Wu S C, Doong R A. Stability of metal oxide nanoparticles in aqueous solutions[J]. Water Sci. Technol., 2010, 61(1): 127−133.

[14] Li L, Hu L P, Li J, Wei Z D. Enhanced stability of Pt nanoparticle electrocatalysts for fuel cells[J]. Nano Res, 2015, 8(2): 418−440.

[15] Kakati N, Maiti J, Lee S H, Jee S H, Viswanathan B, Yoon Y S. Anode catalysts for direct methanol fuel cells in acidic media: do we have any alternative for Pt or Pt-Ru?[J]. Chem. Rev., 2014, 114(24): 12397−12429.

[16] Xiong L K, Sun Z T, Zhang X, Zhao L, Huang P, Chen X W, Jin H D, Sun H, Lian Y B, Deng Z, Rümmerli M H, Yin W J, Zhang D, Wang S, Peng Y. Octahedral gold-silver nanoframes with rich crystalline defects for efficient methanol oxidation manifesting a co-promoting effect[J]. Nat. Commun., 2019, 10: 3782.

[17] Zhang Z Q, Liu J P, Wang J, Wang Q, Wang Y H, Wang K, Wang Z, Gu M, Tang Z H, Lim J, Zhao T S, Ciucci F. Single-atom catalyst for high-performance methanol oxidation[J]. Nat. Commun., 2021, 12(1): 5235.

[18] Teng X A, Shan A X, Zhu Y C, Wang R M, Lau W M. Promoting methanol-oxidation-reaction by loading PtNi nano-catalysts on natural graphitic-nano-carbon[J]. Electrochim Acta, 2020, 353: 136542.

[19] Meng Y, Wang H L, Dai Y H, Zheng J W, Yu H, Zhou C M, Yang Y H. Modulating the electronic property of Pt nanocatalyst on rGo by iron oxides for aerobic oxidation of glycerol. [J]. Catal. Commun., 2020, 144: 106073.

[20] Chen A C, Holt-hindle P. Platinum-based nanostructured materials: synthesis, properties, and applications[J]. Chem. Rev., 2010, 110(6): 3767−3804.

[21] Guo C X, Zhang L Y, Miao J W, Zhang J T, Li C M. DNA-functionalized graphene to guide growth of highly active Pd nanocrystals as efficient electrocatalyst for direct formic acid fuel cells[J]. Adv. Energy Mater., 2013, 3(2): 167−171.

[22] Wang Z H, Xie W F, Zhang F F, Xia J F, Gong S D, Xia Y Z. Facile synthesis of PtPdPt nanocatalysts for methanol oxidation in alkaline solution[J]. Electrochim. Acta, 2016, 192: 400−406.

[23] Li Y J, Sun Y J, Qin Y N, Zhang W Y, Wang L, Luo M C, Yang H, Guo S J. Recent advances on water-splitting electrocatalysis mediated by noble-metal-based nanostructured materials[J]. Adv. Energy Mater., 2020, 10(11): 1903120.

[24] Yuan X L, Jiang B, Cao M H, Zhang C Y, Liu X Z, Zhang Q H, Lyu F L, Gu L, Zhang Q. Porous Pt nanoframes decorated with $Bi(OH)_3$ as highly efficient and stable electrocatalyst for ethanol oxidation reaction[J]. Nano Res., 2020, 13(1): 265−272.

[25] Zhang K F, Wang H F, Qiu J, Wu J A, Wang H J, Shao J W, Deng Y Q, Yan L F. Multi-dimensional Pt/$Ni(OH)_2$/nitrogen-doped graphene nanocomposites with low platinum content for methanol oxidation reaction with highly catalytic performance[J]. Chem. Eng. J., 2021, 421: 127786.

[26] Sideris P J, Nielsen U G, Gan Z H, Grey C P. Mg/Al ordering in layered double hydroxides revealed by multinuclear NMR spectroscopy[J]. Science, 2008, 321(5885): 113−117.

[27] Zhou D J, Li P S, Lin X, McKinley A, Kuang Y, Liu W, Lin W F, Sun X M, Duan X. Layered double hydroxide-based electrocatalysts for the oxygen evolution reaction: identification and tailoring of active sites, and superaerophobic nanoarray electrode assembly[J]. Chem. Soc. Rev., 2021, 50(15): 8790−8817.

[28] Zhou D J, Wang S Y, Jia Y, Xiong X Y, Yang H B, Liu S, Tang J L, Zhang J M, Liu D, Zheng L R, Kuang Y, Sun X M, Liu B. NiFe hydroxide lattice tensile strain: enhancement of adsorption of oxygenated intermediates for efficient water oxidation catalysis[J]. Angew. Chem. Int. Ed., 2019, 58(3): 736−740.

[29] Li P S, Wang M Y, Duan X X, Zheng L R, Cheng X P, Zhang Y F, Kuang Y, Li Y P, Ma Q, Feng Z X, Liu W, Sun X M. Boosting oxygen evolution of single-atomic ruthenium through electronic coupling with cobalt-iron layered double hydroxides[J]. Nat. Commun., 2019, 10: 1711.

[30] Zhou D J, Xiong X Y, Cai Z, Han N N, Jia Y, Xie Q XD, Duan X X, Xie T H, Zheng X L, Sun X M, Duan X. Flame-engraved nickel-iron layered double hydroxide nanosheets for boosting oxygen evolution reactivity[J]. Small Methods, 2018, 2(7): 1800083.

[31] Feng H P, Yu J F, Tang L, Wang J J, Dong H R, Ni T, Tang J, Tang W W, Zhu X, Liang C. Improved hydrogen evolution activity of layered double hydroxide by optimizing the electronic structure[J]. Appl. Catal. B., 2021, 297: 120478.

[32] Han Y C, Li P F, Liu J, Wu S L, Ye Y X, Tian Z F, Liang C H. Strong Fe^{3+}-O(h)-Pt interfacial interaction induced excellent stability of Pt/NiFe-LDH/rGO electrocatalysts[J]. Sci Rep., 2018, 8: 1359.

[33] Zhang J F, Liu J Y, Xi L F, Yu Y F, Chen N, Sun S H, Wang W C, Lange K M, Zhang B. Single-atom Au/NiFe layered double hydroxide electrocatalyst: probing the origin of activity for oxygen evolution reaction[J]. J. Am. Chem. Soc., 2018, 140(11): 3876−3879.

[34] Zhu H Y, Gu C D, Ge X, Tu J P. Targeted growth of Pt on 2D atomic layers of Ni-Al hydroxide: assembly of the Pt/exfoliated Ni-Al hydroxide sheet/graphene composite as electrocatalysts for methanol oxidation reactions[J]. Electrochim. Acta, 2016, 222: 938−945.

[35] Ishikawa Y, Liao M S, Cabrera C R. Energetics of H_2O dissociation and CO_{ads}+OH_{ads} reaction on a series of Pt-M mixed metal clusters: a relativistic density-functional study [J]. Surf Sci, 2002, 513(1): 98−110.

[36] Fan G L, Li F, Evans D G, Duan X. Catalytic applications of layered double hydroxides: recent advances and perspectives[J]. Chem. Soc. Rev., 2014, 43(20): 7040−7066.

[37] Li P S, Duan X X, Kuang Y, Li Y P, Zhang G X, Liu W, Sun X M. Tuning electronic structure of NiFe layered double hydroxides with vanadium doping toward high efficient electrocatalytic water oxidation[J]. Adv. Energy Mater., 2018, 8(15): 1703341.

[38] Xie F, Ma L, Gan M Y, He H M, Hu L Q, Jiang M H, Zhang H H. One-pot construction of the carbon spheres embellished by layered double hydroxide with abundant hydroxyl groups for Pt-based catalyst support in methanol electrooxidation[J]. J. Power Sources, 2019, 420: 73−81.

[39] Lin Y H, Cui X L, Yen C, Wai C M. Platinum/carbon nanotube nanocomposite synthesized in supercritical fluid as electrocatalysts for low-temperature fuel cells[J]. J. Phys. Chem. B., 2005, 109(30): 14410−14415.

[40] Tao L, Shi Y L, Huang Y C, Chen R, Zhang Y Q, Huo J, Zou Y Q, Yu G, Luo J, Dong C L, Wang S Y. Interface engineering of Pt and CeO_2 nanorods with unique interaction for methanol oxidation[J]. Nano Energy, 2018, 53: 604−612.

[41] Huang L, Zhang X P, Wang Q Q, Han Y J, Fang Y X, Dong S J. Shape-control of Pt-Ru nanocrystals: tuning surface structure for enhanced electrocatalytic

methanol oxidation[J]. J. Am. Chem. Soc., 2018, 140(3): 1142−1147.
[42] Tian H, Yu Y H, Wang Q, Li J, Rao P, Li R S, Du Y L, Jia C M, Luo J M, Deng P L, Shen Y J, Tian X L. Recent advances in two-dimensional Pt based electrocatalysts for methanol oxidation reaction[J]. Int. J. Hydrog. Energy, 2021, 46(61): 31202−31215.
[43] Bai G L, Liu C, Gao Z, Lu B Y, Tong X L, Guo X Y, Yang N J. Atomic carbon layers supported Pt nanoparticles for minimized CO poisoning and maximized methanol oxidation[J]. Small, 2019, 15(38): 1902951.
[44] Zhou D J, Cai Z, Bi Y M, Tian W L, Luo M, Zhang Q, Xie Q X, Wang J D, Li Y P, Kuang Y, Duan X, Bajdich M, Siahrostami S, Sun X M. Effects of redox-active interlayer anions on the oxygen evolution reactivity of NiFe-layered double hydroxide nanosheets[J]. Nano Res., 2018, 11(3): 1358−1368.
[45] Cai Z, Zhou D J, Wang M Y, Bak S M, Wu Y S, Wu Z S, Tian Y, Xiong X Y, Li Y P, Liu W, Siahrostami S, Kuang Y, Yang X Q, Duan H H, Feng Z X, Wang H L, Sun X M. Introducing Fe^{2+} into nickel-iron layered double hydroxide: local structure modulated water oxidation activity[J]. Angew. Chem., Int. Ed., 2018, 57(30): 9392−9396.
[46] van Drunen J, Pilapil B K, Makonnen Y, Beauchemin D, Gates B D, Jerkiewicz G. Electrochemically active nickel foams as support materials for nanoscopic platinum electrocatalysts [J]. ACS Appl. Mater. Inter., 2014, 6(15): 12046−12061.

层状金属氢氧化物中铁位点辅助分散铂纳米颗粒用于高效甲醇氧化

孟庆成[a]，金林薄[a]，马梦泽[a]，高学庆[b]，陈爱兵[b,*]，周道金[a,*]，孙晓明[a,*]
[a]化工资源有效利用国家重点实验室，北京化工大学软物质科学与工程高精尖创新中心，北京 100029
[b]河北科技大学化学与制药工程学院，河北 石家庄 050018

摘要

高活性和耐用性的甲醇氧化电催化剂对于直接甲醇燃料电池的商业可行性至关重要，然而，目前的甲醇氧化电催化剂与预期相去甚远，存在贵金属用量过多、活性平庸、衰减快等问题。在这里，我们报告了锚定在镍铁层状金属氢氧化物（NiFe-LDHs）表面 Pt 纳米颗粒复合材料，用于在碱性介质中稳定电催化甲醇氧化。基于 Pt 纳米颗粒的高固有甲醇氧化活性，与商业 Pt/C 催化剂相比，基底材料 NiFe-LDHs 在 200,000 s 循环测试后进一步增强了 Pt 的抗中毒能力和稳定性。NiFe-LDHs 层板上单原子分散的 Fe 作为锚定位点将 Pt 纳米颗粒均匀分散在其表面，进一步充分利用了层状金属氢氧化物表面丰富的 OH 基团，促进邻近 Pt 位点上毒化中间体的氧化去除。这项工作突出了 NiFe-LDH 在提高甲醇氧化反应整体效率方面的特殊性，为其他甲醇氧化电催化的设计和应用提供了指导。

关键词：层状金属氢氧化物；甲醇氧化；单原子；Pt 电催化剂